Simulation of electromechanical actuators with ballscrew and modelling of faults

Jason Wander Cóndor Romero, Álvaro Díaz Campillejo and Amador Gómez Hidalgo
Escuela Técnica Superior de Ingeniería, Universidad de Sevilla, Seville, Spain, 41092

Abstract

In the aerospace field, conventional hydraulic actuators are increasingly being substituted for electrical actuators because they are heavy, inefficient and require a high maintenance. However, electrical actuator technology is energy-efficient and maintainable due to the significant reduction in components. Since it is more interesting to develop a compact structure with no hydraulic components, in this paper it is considered an electromechanical actuator (EMA) instead of an electro-hydrostatic actuator (EHA). EMA technology is not fully realiable due to many mechanical faults. One of the most attractive ways to overcome these problems is the implementation of a health monitoring system. Jamming and backlash have been modelled in Simulink in order to get results which allow a more efficient maintenance and the prevention of major failures.

I. Introduction

Aerospace industry has two main goals to face in future civilian aircrafts designs: create a safer air transport and reduce fuel consumption. Achieving this last target is not only necessary to reduce costs, but also to make "greener" aviation operations in order to reduce carbon footprint[1]. A well known concept related to all these concerns is the "More Electric Aircraft" (MEA). One of the most important bases of MEA is the tendency of replacing the hydraulic actuators by electrical actuation systems ("Power-by-Wire"). The first ones can transmit large forces but they are heavy, inefficient and require a high maintenance. However, electrical actuator technology is energy-efficient and maintainable due to the significant reduction in components[2]. Therefore, this implies a more reliable system.

Electric actuators are controlled, as well as powered, by an electric source[3]. Two types of electric actuators have been introduced in the latest commercial programmes in accordance Ref 1.:

- Electro-hydrostatic actuators (EHAs) as backup actuators for primary and secondary flight controls in the Airbus A380/A400M/A350. For example, A380 achieved a weight reduction of 1500 kg [4]. EHAs still use hydraulics locally to maintain the principal benefits of conventional actuators.
- Electromechanical actuators (EMAs) as frontline actuators for several secondary flight controls, landing gear braking and part of the environmental control system in the Boeing B787. EMAs remove all hydraulic circuits. The EMA modelled in this paper transmits motor power to the load through a ballscrew. Other types of mechanical reducers can be used as a gearbox.

EMAs have some advantages respect to the EHAs: they are smaller and lighter because the only type of energy transformation (electrical to mechanical) allows a compact structure with no hydraulic components. This also means an easy maintenance. Nevertheless, EMA configuration is not a mature technology and presents limitations that are preventing them from being used in primary flight control surfaces in a successful way[4]. The most important restriction has a mechanical nature. For this reason, this paper contains a simulation which studies faults related to the ballscrew: jamming and backlash. On the one hand, the recirculating jam of rotating elements can be caused by degradation of rolling element surfaces due to wear or lubrication failure[5]. On the other hand, the wear of the mechanical transmission components may induce control surface free-play or other non-linearity, which may generate oscillations in the displacement of the actuator rod or unacceptable limit cycles[6]. This is known as backlash and it is graphically described in Fig. 2

One of the most attractive ways to overcome these problems is the implementation of a a health monitoring system. It can be developed by the FFT algorithm or by other techniques, as the ones based on temperature. Thanks to that post analysis, an alarm or a detail prognostics would lead savings in maintenance or even could avoid a catastrophic event[2,5].

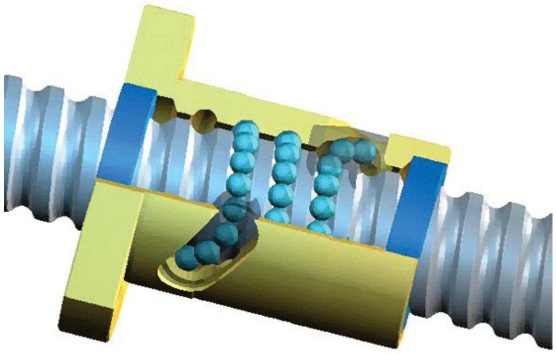

Fig. 1 General view of the ballscrew reducer

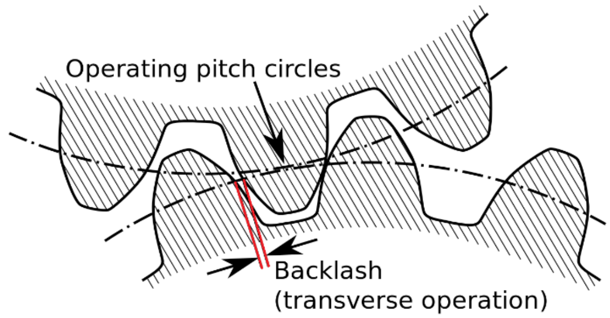

Fig. 2 Backlash description

II. Electromechanical actuator model

In this paper, the EMA model consists of the following components:

- Actuator control electronics (ACE) which perform closed loop position control.
- Power drive electronics (PDE) which control the amount of power flowing between the electrical supply and the motor.
- The electric motor (EM) that transforms power between the electrical and the mechanical rotational domains.
- The ballscrew (BS) mechanical transmission that transforms power between the high speed/low torque rotational and the low velocity/high force translational domains.

In the Fig. , the EMA model and the input/output variables of each block are illustrated.

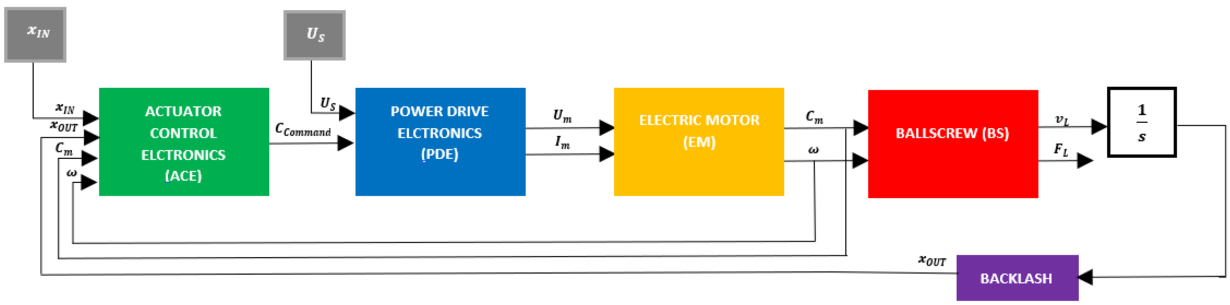

Fig. 3 EMA model (upper level)

The control variable is the desired position, which is considered as a senodial signal. The ACE inputs are desired position x_{IN}, real position x_{OUT}, supplied torque C_m and angular velocity ω. The ACE provides the necessary torque $C_{Command}$ to achieve the desired position. The PDE supplies the proper voltage and current, U_m and I_m respectively, to the electric motor. The motor transforms the electrical power into mechanical. Therefore, the supplied torque and angular velocity, which are tramsmitted to the BS by the electric motor, produce the actuator movement.

All components are modelled in Simulink in accordance each block model, which are explained in following sections.

A. Actuator control electronics (ACE)

The ACE model consists of two PID controller and two mechanical limitations, rotational speed and toque limits, Fig. . Therefore, angular velocity and the supplied torque are nessesary inputs of ACE block.

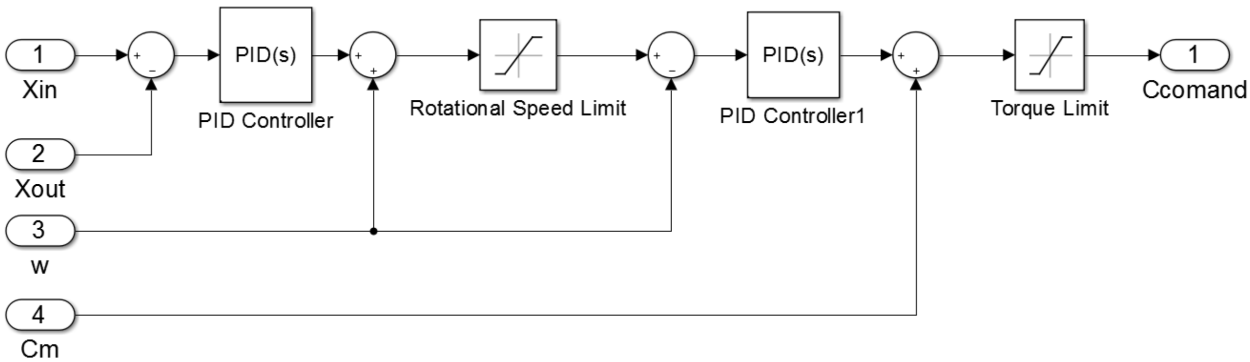

Fig. 4 Simulink model of ACE block

B. Power drive electronics (PDE)

In this case, PDE is considered as a perfect converter with a delay through a second order transfer function according to Eq.(1). Both voltage and current are converted without losses, Fig. 5,

$$C^* = \frac{\omega_i^2}{s^2 + 2\xi_i\omega_i s + \omega_i^2} C_{command} \tag{1}$$

where s is the Laplace variable, and the selected values for the loop natural frequency ω_i and the adimensionless damping factor ξ_i are showed in Table 1.

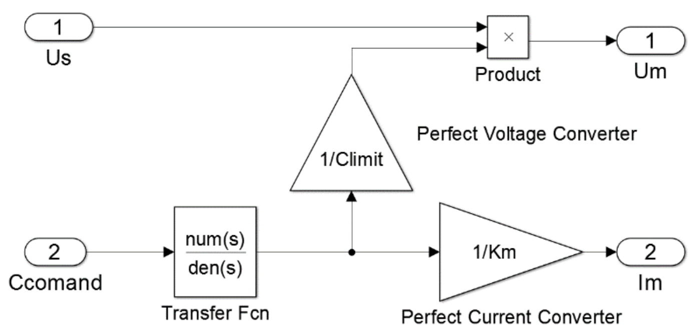

Fig. 5 Simulink model of PDE block

C. Electric motor (EM)

The electric motor is an electromechanical power transformer that functionally links current to torque and voltage to velocity. The perfect power converter is modelled in accordance following equations:

$$C_m = K_m I_m \tag{2}$$
$$\omega_m = U_m / K_m \tag{3}$$

where K_m is the motor electromagnetic constant (N.m/A). However, there are several losses when EM converts. Losses, which have been considered in this case, can be classified into two groups.

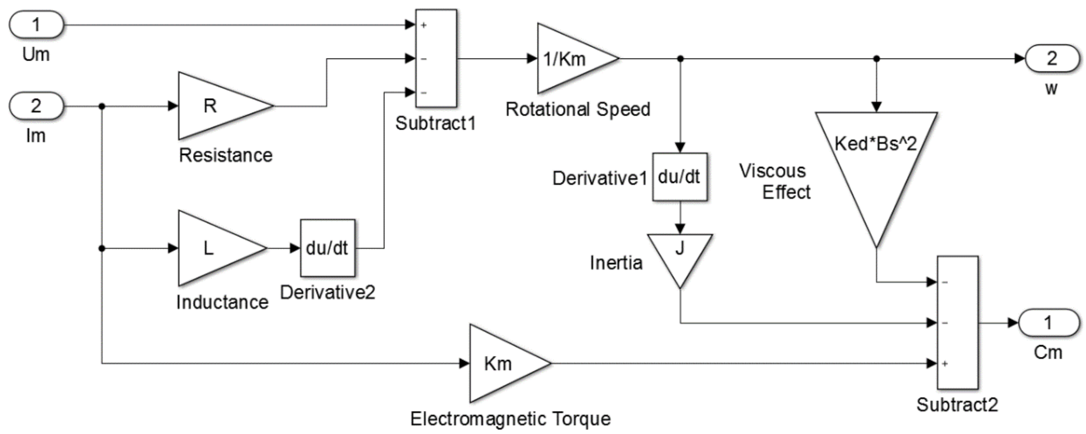

Fig. 6 Simulink model of EM block

1. *Voltage losses:*

These losses reduce the available voltage that is transformed into rotational rod speed. In this case, there are two kinds: Resistance and inductance motor losses.

$$U_{Resistance} = I_m R_{Resistance} \tag{4}$$
$$U_{Inductance} = L_{inductance}\frac{dI_m}{dt} \tag{5}$$

2. *Torque losses:*

These losses reduce the available torque. There are two effects that generate losses: Inertial and Foucault effects. Foucault effect is modelled as a function of the eddy current constant k_{ed}, the magnetic flux density B_s and the angular velocity ω_m.

$$C_{Inertial} = J_m\frac{d\omega_m}{dt} \tag{6}$$
$$C_{Foucault} = k_{ed}B_s^2\omega_m \tag{7}$$

where J_m is the rotor inertia.

D. Ballscrew (BS)

This block is based in a perfect model which achieves pure power transformation between electric motor and the ballscrew[1,7].

$$F_L = 2\pi C_m/p \tag{8}$$
$$V_L = p\omega_m/2\pi \tag{9}$$

In adittion, friction losses are studied[1]. There are numerous types of friction model; however, in this papper only two diferent models are considered:

1. *Simplified velocity dependent model*

$$F_f = f_e \cdot v_r \tag{10}$$

where F_f is the ballscre friction force, f_e is the coefficient of viscous friction and v_r is the tangential velocity.

2. *Velocity and load dependent model*[8]

$$F_f = \left(F_{cl} + F_{st}e^{-|v_r|/v_{st}} + |F_L|\left(a + bsgn(F_L v_r)\right)\right) sgn(v_r) \tag{11}$$

Where F_{cl} and F_{st} respectively are the Coulomb force and the Stribeck force, v_{st} is the Stribeck reference velocity, a is the mean coefficient of external force and b is the quadrant coefficient.

The effects of friction in velocity is modelled by a efficiency coefficient as is illustrated in Fig. 7.

The backlash is inserted into de signal line of position after the integration of velocity in order to model the behavior of the mechanical play.

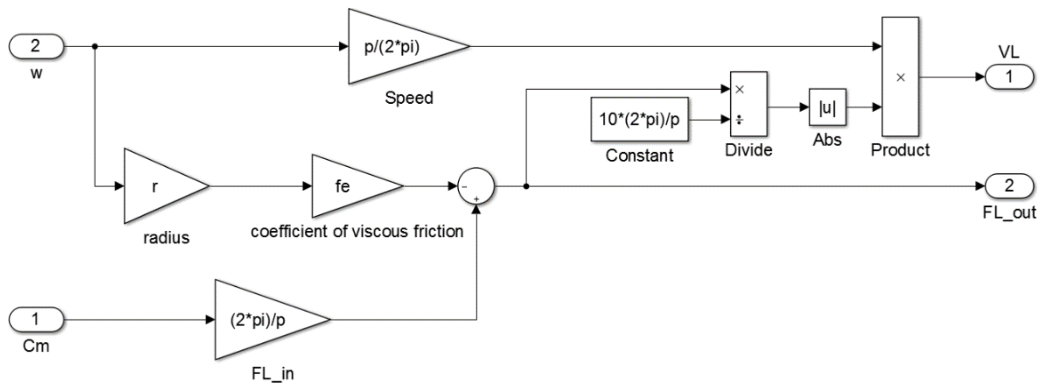

Fig. 7 Simulink model of Ballscrew

III. Model simulation for faults detection

The response to failure of EMAs has been simulated through the model described above. The simulation is focus on mechanical faults because these kinds of faults are preventing the implementation of this actuator in the primary flight control surfaces in a successful way. For this reason this simulation studies faults which happen in the ballscrew block: jamming and increased backlash. Jamming can be modelled by increasing parameter values of the friction model. This rise of friction leads EMA to stop when the effect of jamming is too high. Regarding backlash, it can be analized by modifying the deadband width in backlash block.

Table 1 EMA controller and motor parameters

Parameter	Value
Position loop proportional gain K_p $(rad \cdot s^{-1} \cdot m^{-1})$	4500
Velocity loop proportional gain K_v $(N \cdot m \cdot s/rad)$	0.5
Velocity demand saturation ω_{lim} (rad/s)	314
Torque demand saturation C_{lim} $(N \cdot m)$	10
DC supply voltage U_s (V)	200
Loop natural frequency ω_i (rad/s)	12.5664
Adimensionless PDE damping factor ξ_i	1
Motor resistance R (Ω)	1.77
Motor inductance I (H)	0.00678
Magnetic flux density B_s (T)	2
Rotor inertia J $(kg \cdot m^2)$	0.00171
Torque constant K_m $(N \cdot m/A)$	1.65
Constant of eddy current loss K_{ed}	9.3×10^{-6}

Table 2 EMA ballscrew parameters

Parameter	Value
Lead of screw p (mm)	2.54
Coefficient of viscous friction f_e $(N/(m \cdot s^{-1})$	10
Backlash deadband width b (m)	2×10^{-5}
Screw radius r (m)	0.05

A. Ideal model

In order to be able to compare results when there is a failure, the model has been simulated without fails using starting parameters showed in Table 1-2. These parameters are based on Ref 1. In these simulations the simplified friction model has been used with the aim of not getting too computer time cost. The position commanded is a sine with 50mm of amplitude and 1 rad/s of frequency. This signal lets a post analysis using the FFT algorithm.

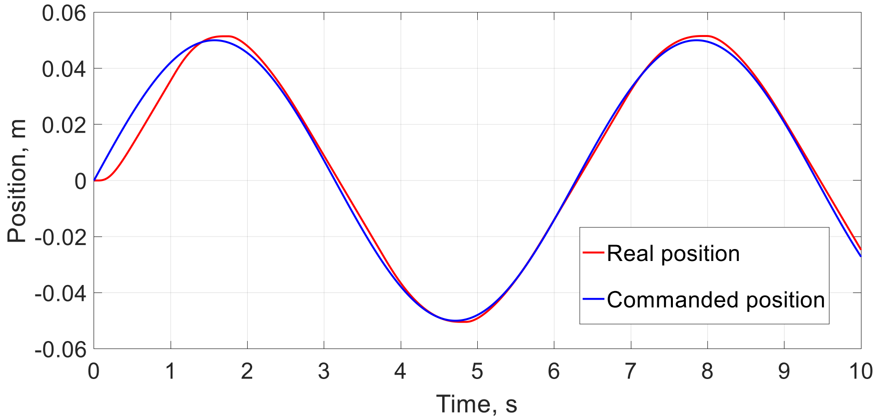

Fig. 8 Position response of model and commanded position

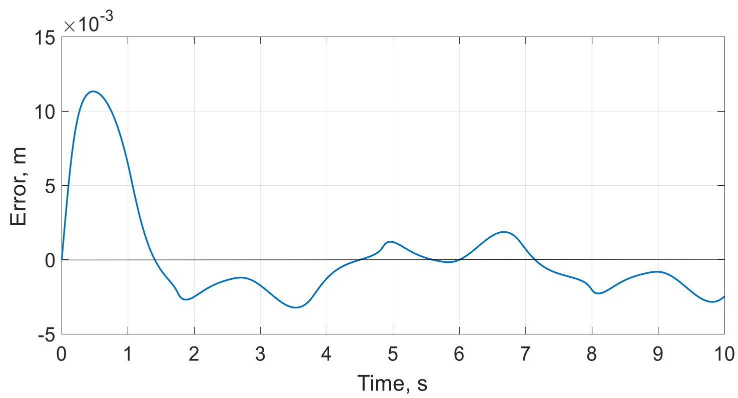

a) Error between the real position and the desired position

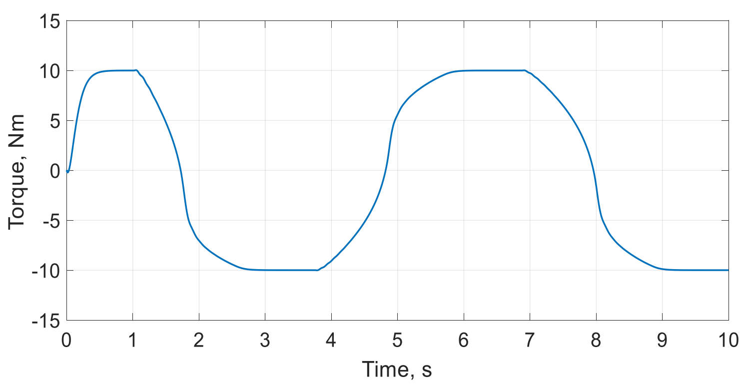

b) Torque response

Fig. 9 Results of simulation of model without faults

The curves of Fig. 8 show the real position and the desired position in the model without faults. Despite the error at the beginning due to the delay in PDE, the biggest difference between the real position and the commanded position happens when the torque demand saturation is achieved (time 3.5 s and 6.5 s). Indeed that effect is shown in Fig. 9(a) where the error is displayed and in Fig. 9(b) where the torque response is illustrated.

It is necessary to study the acceleration response of EMA; therefore, spectrum analysis of the acceleration is displayed with the acceleration in Fig. 10.

B. Backlash failure

Three diferent cases of backlash deadband width have been studied in addition to the ideal case. The first case, $b = 5 \times 10^{-4}\, m$, corresponds to a degraded work: the actuator is able to continue working but in a less efficient way. The second case would imply an early detection of the failure and a maintenance in time. Finally the third case, backlash deadband width equal to 10% of the amplitude commanded, will mean a significative error and the necessity of an urgent maintenance. These cases are illustrated in Fig. 11

The spectrum analysis of acceleration in Fig. 12(a) shows a spike in a frecuency of 5 Hz and that spike approachs to the fundamental frequency when backlash increases. Therefore, it is possible to detect a backlash failure by monitoring the spectrum response of acceleration, the failure will happen when the second spike exceeds 50% of fundamental magnitude.

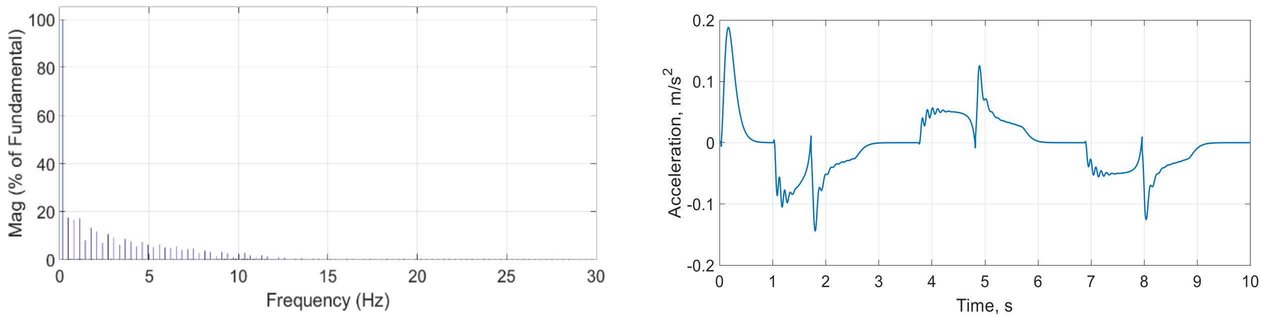

a) Acceleration FFT

b) Acceleration versus time

Fig. 10 Acceleration response of model without failure

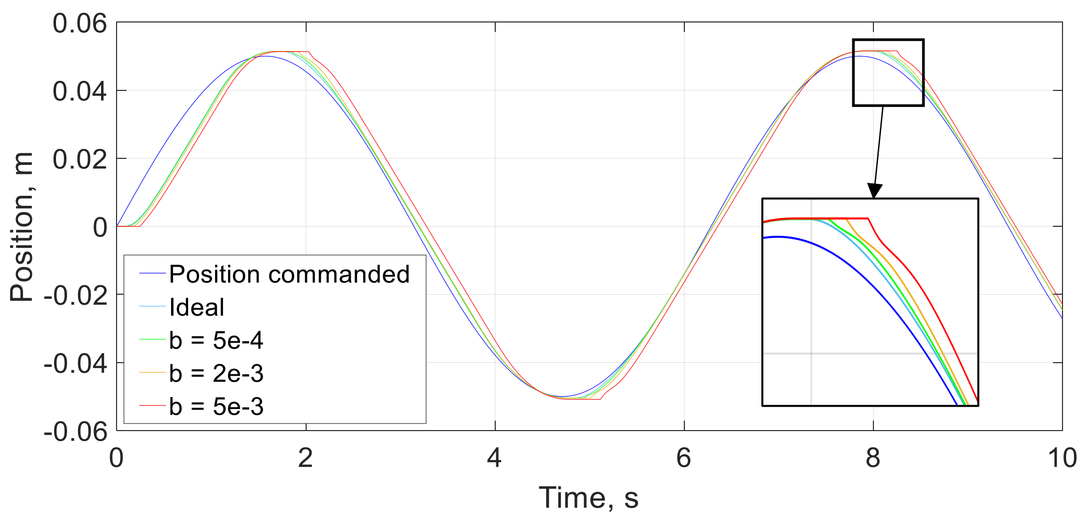

Fig. 11 Position response with different backlash deadband

C. Jamming failure

Again, three states of jamming have been studied. None of them is a total jam although the last case is very similar to a total jam because the displacement of this state is very low. In the first case, the coefficient of viscous friction is rather high as compared with ideal case, nevertheless the position response is very similar. These curves are displayed in Fig. 13(a).

A suitable health monitoring system should detect the presence of jamming before the coefficient of viscous friction reaches the value of first case $f_e = 500\ N/(m \cdot s^{-1})$ because if jamming is detected very late, it could cause a total failure like in the third case. This detection through FFT is not so easy as backlash because the effects on spectrum analysis appear later. In Fig. 13(c) there are waves which are more important than in Fig. 13(b) where jamming is less significant. That means that the detection could be too later. It would be interesting to use a thermocouple and a thermal model to be able to preview jamming better. Jamming produces a rise of temperature due to friction and that effect would be registered by the thermocouple in order to detect the failure.

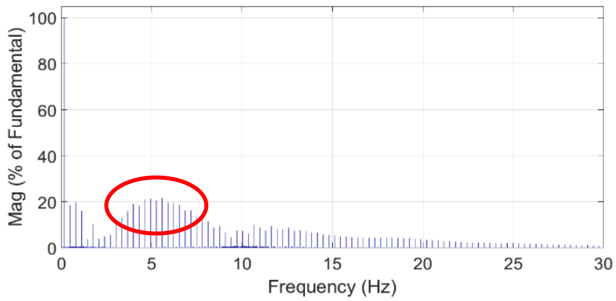

a) Backlash deadband width = $5x10^{-4}\ m$

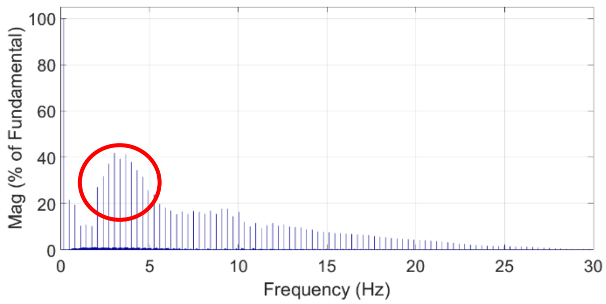

b) Backlash deadband width = $2x10^{-3}\ m$

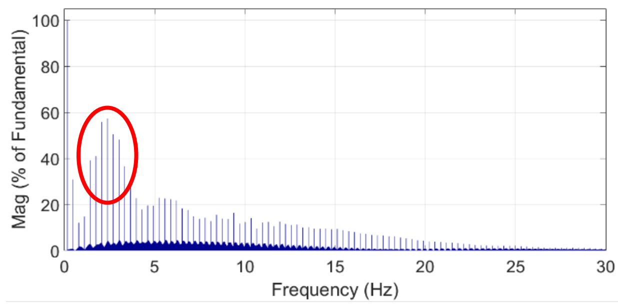

c) Backlash deadband width = $5x10^{-3}\ m$

Fig. 12 Time and FFT analysis of backlash

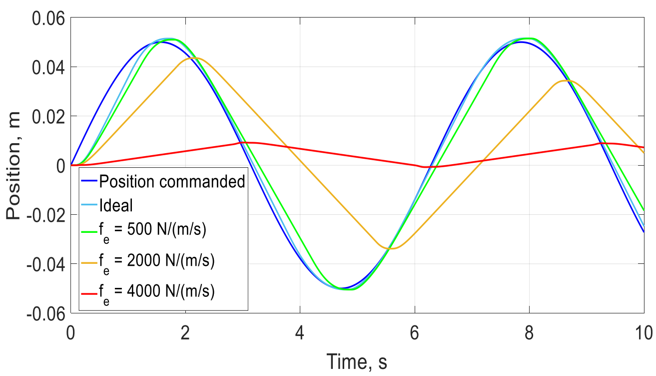

a) Position response with jamming failure

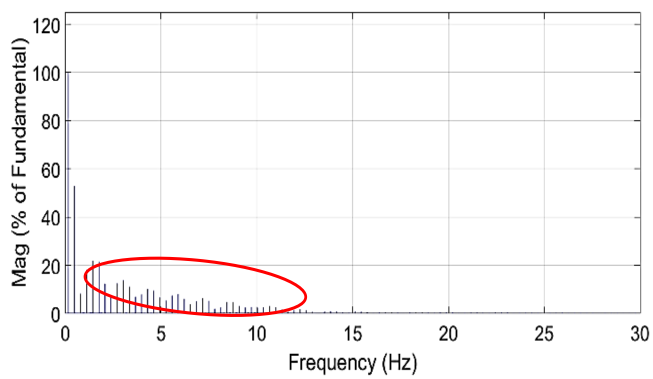

b) FFT $f_e = 500\ N/(m/s)$

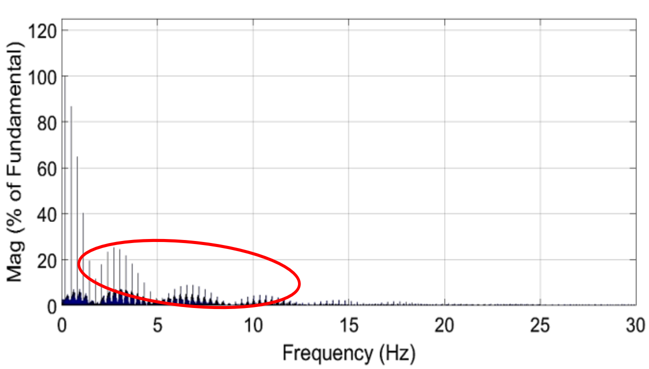

c) FFT $f_e = 2000\ N/(m/s)$

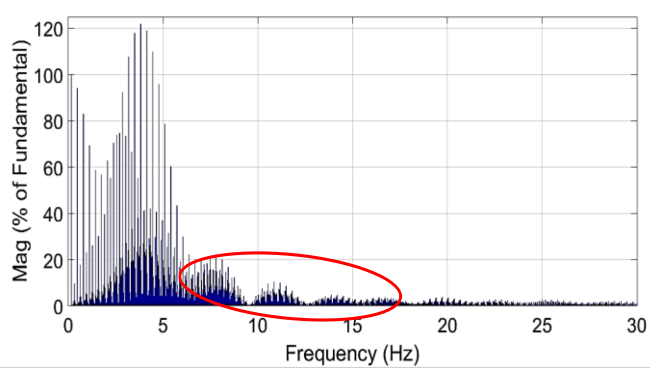

d) FFT $f_e = 4000\ N/(m/s)$

Fig. 13 Time and FFT analysis of jamming

IV. Conclusion

In the perspective of the More Electric Aircraft, a current challenge is the implementation of EMAs instead of hydraulic devices. For this reason, the research developed in this paper was focused on the main problems that present these actuators: mechanical faults, in particular, backlash and jamming. In order to implement a health monitoring system, it has been used FFT analysis to know the state of the actuator with respect to these two types of failure. Through the frequency spectrum, it is possible to anticipate failures and improve preventive maintenance. Nevertheless this is not very reliable for jamming detection so it would be necessary an alternative method as a thermal model.

This study has been done by simulation, however it would be recommendable to experiment with a real actuator in order to compare the model used here with the reality and check if a health monitoring system and the failures would behave like in this paper.

References

[1] Fu Jian, Jean-Charles Maré and Fu Yongling, "Modelling and simulation of fligh control electromechanical actuators with special focus on model architecting, multidisciplinary effects and power flows," CSAA, 2016.

[2] J.-C. Derrien, "Electromechanical actuator (EMA) advanced technologies for flight controls," ICAS, 2012 conference proceedings.

[3] Mohamed A.A. Ismail, Edward Balaban and Holger Spangenberg, "Fault detection and classification for flight control electromechanical actuators", IEEE, 2016.

[4] C. Adams "A380: More Electric Aircraft", Avionics Magazine, Oct 2001.

[5] Rosa María Basagoiti, Eduardo de la Torre and othes, "Development of an aeronautical electromechanical actuator with real time health monitoring capability", Recent Advances in Aerospace Actuation Systems and Components Conference, Toulouse , 2010.

[6] Michael Todeschi and Laura Baxerres, "Health monitoring for the flight control EMAs", IFAC, 2015

[7] Jianyong Y, Wenxiang D and Zongxia J. "Adaptive control of hydraulic actuators with LuGre model-based friction compensation" IEEE Trans Ind Electron 2015;62(10):6469–77.

[8] Karam W and Maré J-C. "Modelling and simulation of mechanical transmission in roller-screw electromechanical actuators," Aircr Eng Aerosp Technol 2009;81(4):288–98.